PHYSICAL REVIEW B VOLUME 8, NUMBER 12 15 DECEMBER 1973

# Phonon Frequencies and Cohesive Energies of Copper, Silver, and Gold

Natthi Singh and Satya Prakash
*Physics Department, Panjab University, Chandigarh, India*
(Received 21 May 1973)

The static dielectric functions of copper, silver, and gold are investigated in the noninteracting band scheme using the exchange-correlation corrections due to Singwi *et al.* in the *s-s* part of the dielectric function. These dielectric functions are further used in conjunction with Harrison's model potential to investigate the electronic contribution to the phonon frequencies. The direct ion-ion-interaction contribution to phonon frequencies is evaluated by Ewald's method and the contribution due to exchange-overlap potential is calculated using an overlap potential calculated by Moriarty. The calculated phonon frequencies for copper and silver along the three principal symmetry directions [100], [110], and [111] are in good agreement with experimental values except for transverse branches in the [100] and [110] directions for copper. The results for gold are compared with the calculations of Moriarty. The effective ion-ion potential and form factors for all these metals are also calculated. The calculated cohesive energies of these metals are in poor agreement with the experimental values while good agreement is obtained with the calculations of Moriarty for silver and gold.

## I. INTRODUCTION

There has been lot of interest in the investigation of lattice dynamical properties of noble metals by a first-principles approach. Toya[1] had initiated this approach by calculating the phonon frequencies of copper, but the method he used was exactly the same as that used for alkali metals. In the discussion of electrical resistivity of transition metals,[2] Toya suggested that the change in charge distribution of conduction electrons, owing to lattice vibrations in these metals, can be divided into two parts. One is the bound part and it can be assumed to move rigidly with the nuclei resulting into the quasi-ion core. The other is the free part and is responsible for the screening of the motion of the quasi-ions. This concept is rigorously formulated by Sinha[3] in the augmented-plane-wave (APW) scheme. Golibersuch[4] also discussed the electron-phonon (EP) interaction in the APW scheme. These schemes seem to be quite suitable for the noble metals, but because of the complicated and involved calculations, these have not been applied to calculate the phonon frequencies of any metal as yet. Das[5] and Nowak[6] also calculated EP interaction for a noble metal, copper, using the Mueller-interpolation scheme[7] and the APW phase-shift-analysis scheme introduced by Ziman,[8] respectively, to calculate the mass enhancement and the relaxation time of the quasiparticles. These formulations have also not been extended to investigate the other properties of these metals.

Harrison[9] reformulated the pseudopotential method and generalized it to *d*-band metals, which has been used by Moriarty to calculate the form factors, phonon frequencies, and the total energies[10,11] of noble metals. The results for phonon frequencies of copper do not show agreement with the experimental values, while the results for silver show only reasonable agreement with the experimental values. Kohn anomalies are also found in the phonon frequencies of copper in the T and $T_1$ branches in the [100] and [110] directions. Moriarty analysis, although founded on a rigorous basis, is extremely intricate and its usefulness may be better appreciated from the conceptual point of view. However, the detailed band-structure effects in the calculation of the dielectric function are not incorporated by Moriarty. Nikulin and co-workers[12] also made a pseudopotential analysis of the cohesive energies of noble metals. They used the Gombas[13] overlap potential between the nearest-neighbor ions and the Heine-Avarankov[14] model potential for the electron-ion interaction. For screening, the Hartree dielectric function modified by exchange-correlation corrections due to Hubbard[15] and Kleinman[16] is used. Though their results for cohesive energy, compressibility, and phonon frequencies are in reasonably good agreement with the experimental values, their use of the free-electron dielectric function is hardly justified for noble metals.

Earlier, a noninteracting band model was proposed to evaluate the static dielectric function of transition metals[17] and was used to calculate the phonon frequencies of paramagnetic nickel[18] and copper[19] (hereafter, Refs. 17, 18, and 19 will be referred to as papers I, II, and III, respectively). The calculated phonon frequencies were found in fair agreement with the experimental values for nickel while for copper, the calculated phonon frequencies for the transverse branches were as low as 30% less than the experimental values for some wave vectors. In paper III, the contribution due to the overlap potential between the ions was completely neglected. The exchange-correlation cor-

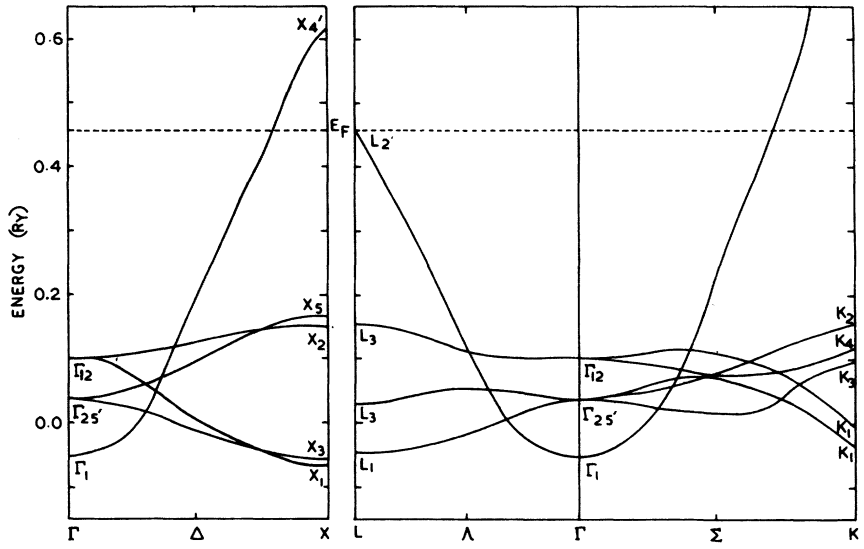


FIG. 1. Noninteracting band model for silver based on the calculations of Snow (Ref. 22). Dashed line shows the Fermi energy.

rections in the dielectric function were also ignored. In the present paper the phonon frequencies and the cohesive energy of copper is reinvestigated using the exchange-overlap potential between the ions calculated by Moriarty[11] and including the exchange-correlation corrections due to Singwi *et al.*[20] in the *s-s* part of the dielectric function. A similar scheme is applied to silver and gold. The effective ion-ion interaction, form factors, and the cohesive energies of all these metals are also investigated.

In Sec. II, we briefly review the construction of the isotropic noninteracting band model. Sections III and IV are devoted to the calculations of the dielectric function and the phonon frequencies. The effective ion-ion interaction, form factors, and cohesive energies are presented in Secs. V, VI, and VII, respectively. The results are summarized in Sec. VIII.

## II. ISOTROPIC ENERGY-BAND STRUCTURE

The self-consistent APW band-structure calculations of Snow and Waber,[21] Snow,[22] and Christensen and Seraphin[23] are used to construct the noninteracting band models for copper, silver, and gold, respectively. These models for silver and gold are shown in Figs. 1 and 2, while for copper the same model is used as discussed in paper III.

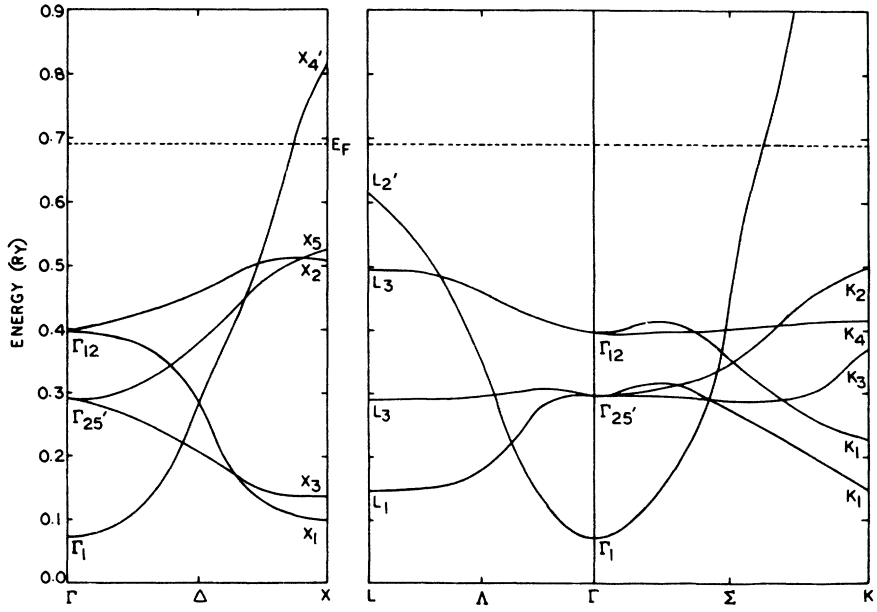


FIG. 2. Noninteracting band model for gold based on the calculations of Christensen and Seraphin (Ref. 23). The description is the same as that of Fig. 1.

TABLE I. $m$ assignment to different $d$ subbands.

| [110] | [110] | [111] | $m$ |
|---|---|---|---|
| $\Gamma_{12} \rightarrow X_2$ | $\Gamma_{12} \rightarrow K_4$ | $\Gamma_{12} \rightarrow L_3$ | 2 |
| $\Gamma_{12} \rightarrow X_1$ | $\Gamma_{12} \rightarrow K_1$ | $\Gamma_{12} \rightarrow L_3$ | 0 |
| $\Gamma_{25'} \rightarrow X_5$ | $\Gamma_{25'} \rightarrow K_2$ | $\Gamma_{25'} \rightarrow L_3$ | 1 |
| $\Gamma_{25'} \rightarrow X_3$ | $\Gamma_{25'} \rightarrow K_3$ | $\Gamma_{25'} \rightarrow L_3$ | −1 |
| $\Gamma_{25'} \rightarrow X_5$ | $\Gamma_{25'} \rightarrow K_1$ | $\Gamma_{25'} \rightarrow L_1$ | −2 |

The magnetic-quantum-number, $m$, assignment to different $d$ subbands and the calculation of isotropic energy bands is done exactly in the same manner as discussed in paper I. For ready reference, the $m$ assignment to different $d$ subbands is given in Table I. The isotropic energy-band structures for silver and gold are shown in Figs. 3 and 4, respectively, while for copper the isotropic energy band structure from paper III is used. The physical parameters used in this calculation and the average effective masses for all the $d$ subbands are given in Tables II and III, respectively. The energy is measured in rydbergs, and the distance is measured in Bohr units.

## III. DIELECTRIC FUNCTION

It is evident from the model band structures that all the $d$ subbands are filled and the Fermi level intersects only the $s$ band. Therefore, the readjustment of the electron in response to the displacement of ions due to lattice vibrations will be caused by the two types of transitions, i.e., from the unfilled $s$ band to unfilled $s$ band and from the filled $d$ subbands to unfilled $s$ bands. Therefore, the dielectric function is written as

$$\epsilon(\vec{p}) = 1 - \epsilon_{ss}(\vec{p}) - \epsilon_{ds}(\vec{p}) , \tag{1}$$

where $\epsilon_{ss}(\vec{p})$ and $\epsilon_{ds}(\vec{p})$ are $-4\pi e^2/p^2$ times the polarizability functions which arise from the intraband and interband transitions, respectively. $\vec{p} = \vec{q} + \vec{G}$, where $\vec{q}$ is the phonon wave vector and $\vec{G}$ is the reciprocal-lattice vector. The detailed derivations of $\epsilon_{ss}(\vec{p})$ and $\epsilon_{ds}(\vec{p})$ are given in paper I and just to introduce the necessary notations, the final expressions for $\epsilon_{ss}(\vec{p})$ and $\epsilon_{ds}(\vec{p})$ are retained here:

$$\epsilon_{ss}(\vec{p}) = -\frac{2m_s k_{Fs} e^2}{\pi\hbar^2 p^2}\left[1 + \frac{4k_{Fs}^2 - p^2}{4k_{Fs}p}\ln\left|\frac{2k_{Fs}+p}{2k_{Fs}-p}\right|\right] \tag{2}$$

and

$$\epsilon_{ds}(\vec{p}) = \frac{32e^2 m_s}{\Omega_0 p^2 \hbar^2}\sum_m (-1)^m \times\left(\int_0^{k_{Fdm}} dk\, k^2 [F_2(k)]^2 [D_{0m}^2 D_{0-m}^2 I_0 + (D_{1m}^2 D_{-1-m}^2 + D_{-1m}^2 D_{1-m}^2) I_1 + (D_{2m}^2 D_{-2-m}^2 + D_{-2m}^2 D_{2-m}^2) I_2]\right) , \tag{3}$$

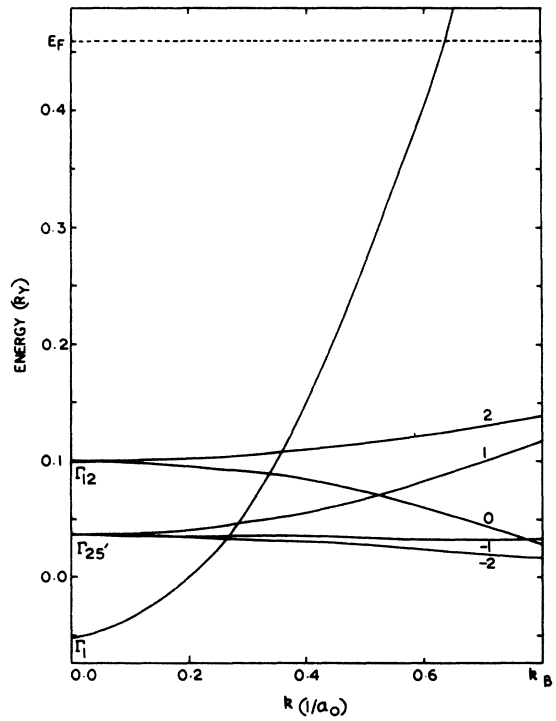


FIG. 3. Isotropic energy band structure for silver. The numbers near the curves denote the magnetic quantum number $m$ assigned to $d$ subbands.

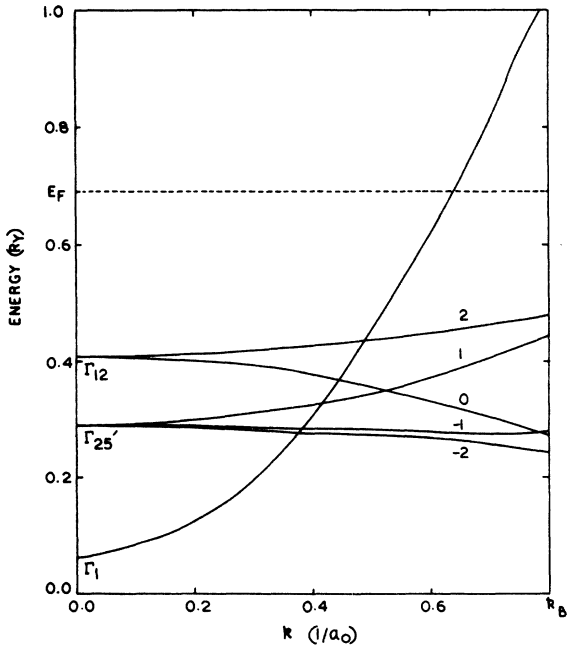


FIG. 4. Isotropic energy band structure for gold. The description is the same as that of Fig. 3.

TABLE II. Physical parameters for noble metals.

| Parameters | Copper | Silver | Gold |
|---|---|---|---|
| Lattice constant $a_l$ (in units of Bohr radius $a_0$) | 6.8309 | 7.7110 | 7.6813 |
| Atomic volume $\Omega_0$ (in units of $a_0^3$) | 79.6835 | 114.615 | 113.35 |
| Radius of the Brillouin sphere $k_B$ (in units of $1/a_0$) | 0.9057 | 0.80264 | 0.8052 |
| Fermi momentum for the $s$ band $k_{Fs}$ (in units of $1/a_0$) | 0.7189 | 0.63665 | 0.6392 |
| Effective mass for the $s$ band $m_s$ (atomic units) | 0.9603 | 0.7929 | 0.6515 |
| Ionicity $Z$ | 1 | 1 | 1 |
| Plasma frequency $\omega_{pl}$ (Hz) | $48.24\times10^{12}$ | $30.85\times10^{12}$ | $22.96\times10^{12}$ |
| $\bar{r}_s$ (bohr) | 2.669 | 3.013 | 3.002 |
| $A$ | 0.940 | 0.978 | 0.978 |
| $B$ | 0.310 | 0.304 | 0.304 |

where

$$m_s = \hbar^2 k_{Fs}^2/2E_F \tag{4}$$

and

$$k_{Fs} = (3\pi^2 z_s/\Omega_0)^{1/3} . \tag{5}$$

$E_F$ is the Fermi energy, $z_s$ is the number of $s$ electrons per atom, $\Omega_0$ is the atomic volume, $e$ is the electronic charge, $D^2_{m',m}$ are the elements of rotation matrix with argument $(-\gamma', -\beta', -\alpha')$, where $\alpha'$, $\beta'$, and $\gamma'$ are the Euler's angles, $\vec{k}$ is electron wave vector, and

$$k_{Fdm} = (3\pi^2 z_{dm}/\Omega_0)^{1/3} , \tag{6}$$

$$I_0 = \tfrac{5}{4}(0.5 I_{n0} - 3 I_{n2} + 4.5 I_{n4}) ,$$

$$I_1 = \tfrac{15}{4}(-I_{n2} + I_{n4}) ,$$

$$I_2 = \tfrac{15}{8}(0.5 I_{n0} - I_{n2} + 0.5 I_{n4}) . \tag{7}$$

Here

$$I_{n0} = -\frac{1}{b}\ln\left|\frac{b-a}{b+a}\right| ,$$

$$I_{n2} = -\frac{1}{b}\left[\frac{2a}{b} + \frac{a^2}{b^2}\ln\left|\frac{b-a}{b+a}\right|\right] ,$$

$$I_{n4} = -\frac{1}{b}\left[\frac{2a}{3b} + \frac{2a^3}{b^3} + \frac{a^4}{b^4}\ln\left|\frac{b-a}{b+a}\right|\right] , \tag{8}$$

$$a = k^2(m_s/m_{dm} - 1) - p^2 , \tag{9}$$

$$b = 2kp . \tag{10}$$

The function $F_2(k)$, which involves the radial part of the $d$ wave function, is defined as

$$F_2(k) = \int_0^\infty j_2(kr) R_d(r) r^2 dr , \tag{11}$$

where $j_2(kr)$ is the spherical Bessel function and the radial part of the $d$ wave function:

$$R_d(r) = \sum_i a_i r^2 e^{-\alpha_i r} , \tag{12}$$

where $a_i$ and $\alpha_i$ are the parameters. Using (12) in (11) one gets

$$F_2(k) = 48k^2 \sum_i \frac{a_i \alpha_i}{(k^2 + \alpha_i^2)^4} . \tag{13}$$

The parameterized $3d$ radial wave functions tabu-

TABLE III. Average effective masses for the $d$ subbands in atomic units.

| | $m$ | 0 | 1 | 2 | −2 | −1 |
|---|---|---|---|---|---|---|
| Copper | $m_{dm}$ | −12.3460 | 14.4214 | 31.8811 | −28.1515[a] | −83.5271 |
| Silver | $m_{dm}$ | −9.1105 | 7.9818 | 16.7442 | −31.0276 | −151.7415 |
| Gold | $m_{dm}$ | −4.81392 | 4.4810 | 8.9228 | −14.0275 | −37.6983 |

[a]There was a small error in the calculation of this value in paper III.

TABLE IV. Parameters of radial wave functions for noble metals.

| | Copper | | Silver | | Gold | |
|---|---|---|---|---|---|---|
| $i$ | $a_i$ | $\alpha_i$ | $a_i$ | $\alpha_i$ | $a_i$ | $\alpha_i$ |
| 1 | 1.4105 | 1.5370 | 1121.4765 | 12.1103 | −10726.521 | 16.3363 |
| 2 | 23.0751 | 3.0624 | 268.6802 | 19.4000 | 4342.4725 | 24.8543 |
| 3 | 125.4921 | 5.7817 | −543.3063 | 11.2508 | 11387.7501 | 15.4451 |
| 4 | 79.6966 | 10.3718 | 123.5029 | 7.3758 | −1426.9265 | 9.1832 |
| 5 | | | −23.0122 | 4.5804 | 582.1242 | 6.4205 |
| 6 | | | −14.1396 | 2.8665 | −266.8762 | 5.2589 |
| 7 | | | | | 33.5970 | 3.0783 |
| 8 | | | | | −2.2167 | 1.9621 |
| 9 | | | | | 0.8090 | 1.4220 |

lated by Watson[24] are used for copper for the atomic condiguration $(3d)^{10}(4s)^1$. Such parameterized $4d$ and $5d$ radial wave functions for silver and gold are not available. Therefore, Herman-Skillman[25] atomic $4d$ and $5d$ radial wave functions are used by fitting them in the analytic form (13) by the generalized least-squares method.[26] These parameters for silver and gold along with those of copper are tabulated in Table IV. The $4d$ and $5d$ radial wave functions obtained by using these sets of parameters are in close agreement with those tabulated by Herman and Skillman as shown in Fig. 5. The maximum deviation is only of the order of 3% for silver for large values of $r$.

In paper I, $\epsilon(\vec{p})$ is evaluated in the Hartree approximation. It is too difficult to include the exchange and correlation corrections in the dielectric function self-consistently in the present scheme. However, these corrections can be incorporated phenomenologically. $\epsilon_{ss}(\vec{p})$, which arises from the $s$-band to $s$-band transitions, is evaluated in the free-electron approximation and several authors[27] have suggested different exchange-correlation corrections for the free particles. The corrections of Singwi *et al.*[20] are found to be the best since these are evaluated self-consistently and yield positive pair correlation functions in the metallic-density region. Incor-

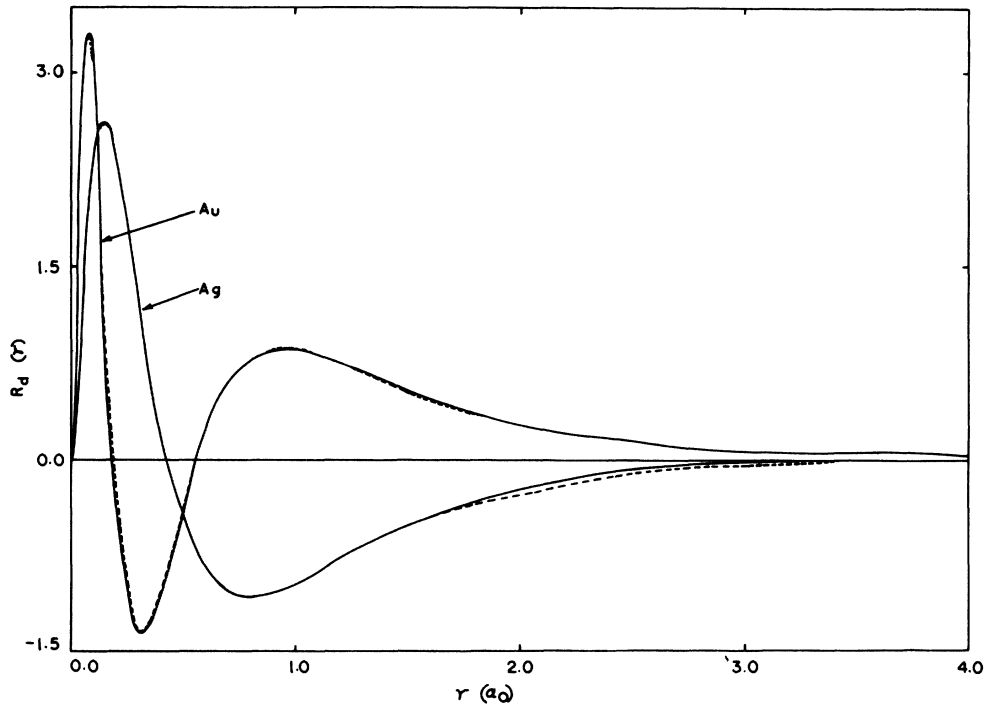


FIG. 5. Comparison of Herman-Skillman and least-square fitted $4d$ and $5d$ radial wave functions for silver and gold, respectively. The solid lines represent the least-square-fitted wave functions and the dashed lines represent the Herman-Skillman wave functions.

porating these corrections we can write the screened $\epsilon_{ss}(\vec{p})$ as

$$\epsilon'_{ss}(\vec{p}) = \frac{\epsilon_{ss}(\vec{p})}{1 - f(p)\epsilon_{ss}(\vec{p})} , \tag{14}$$

where

$$f(p) = A(1 - e^{-B(p/k_{Fs})^2}) . \tag{15}$$

$f(p)$ is the Gaussian fit of the self-consistently calculated exchange-correlation factor. The parameters $A$ and $B$ have been tabulated by Vashishta and Singwi[28] in a recent paper for a set of values of interelectronic distances $\bar{r}_s$. The interelectronic distances for $s$ electrons are 2.669, 3.013, and 3.002 bohr for copper, silver, and gold, respectively. The corresponding parameters $A$ and $B$, which are used in this calculation, are given in Table II. Moriarty[10,11] has also used a similar scheme for exchange-correlation correction among the $s$ electrons. He also used the Kohn-Sham[29] approximation with Lindgren[30] corrections for the exchange between $d$ and $s$ electrons, which we have completely neglected. The $\epsilon_{ds}(\vec{p})$ part arises due to transitions from $d$ subbands to the $s$ band. The electrons in the $d$ subbands are treated in the tight-binding approximation in the present scheme. Therefore, both the free-electron and atomic limits[31] are unsuited for the $d$ electrons in bands of finite width. We, therefore, do not incorporate any correction to the $\epsilon_{ds}(\vec{p})$ part. The interelectronic distances for $d$ electrons are 1.239, 1.395, and 1.394 bohr for copper, silver and gold, respectively. The function $f(p) \to 0$ as $\bar{r}_s \to 1$. This further justifies the neglection of exchange-correlation corrections in the $\epsilon_{ds}(\vec{p})$ part. Therefore, we write the dielectric function defined by Eq. (1) as

$$\epsilon(\vec{p}) = 1 - \epsilon'_{ss}(\vec{p}) - \epsilon_{ds}(\vec{p}) . \tag{16}$$

Here it is to be noted that $\epsilon'_{ss}(\vec{p})$ is isotropic and depends only on the Fermi momentum $k_{Fs}$, while $\epsilon_{ds}(\vec{p})$ is anisotropic and involves an explicit summation over electron wave vectors $\vec{k}$. As was pointed out in I, that because of the choice of the polar axis and the use of spherical harmonics, the dielectric function does not exhibit the crystal symmetry. Therefore $\epsilon(\vec{p})$ is calculated along the directions equivalent to [100], [110], and [111]. For example, $\vec{p}$ is taken along all the six directions equivalent to [100] and the corresponding values of $\epsilon(\vec{p})$ are obtained. For a value of $\vec{p}$, the simple average of all the six values of $\epsilon(\vec{p})$ is taken as the average $\epsilon(\vec{p})$ along [100] direction. Similar procedure is adopted for the calculation of $\epsilon(\vec{p})$ along [110] and [111] directions. We found from our calculations that $\epsilon_{ds}(\vec{p})$ is approximately half of $\epsilon'_{ss}(\vec{p})$ for copper, while for silver it is negligible and for gold $\epsilon_{ds}(\vec{p})$ is about 16% of $\epsilon'_{ss}(\vec{p})$ though the $d$ bandwidths of copper, silver, and gold are in increasing order. The $\epsilon_{ds}(\vec{p})$ depend on the function $R_d(r)$. Because of the nodes of the $d$ radial wave functions for copper, silver, and gold, the function $F_2(k)$ is found quite large for copper and negligible for silver and gold.

The dielectric function calculated with the help of Eq. (16) is shown in the Figs. 6–8 for copper, silver, and gold, respectively, along all the three principal symmetry directions. We find that the anisotropy in the dielectric functions is quite small. To see the effect of exchange-correlation correction, we have also plotted $\epsilon(\vec{p})$ along the [100] direction calculated by Eq. (1) for all the metals. We find that the dielectric functions are enhanced by 90% to 1% in the low-$\vec{p}$ region, while these remain almost unaltered for large values of $\vec{p}$.

## IV. LATTICE DYNAMICS

In the harmonic approximation, the angular frequencies $\omega_{q\rho}$ of lattice vibrations of a monatomic lattice are obtained from the solution of the usual determinantal equation,

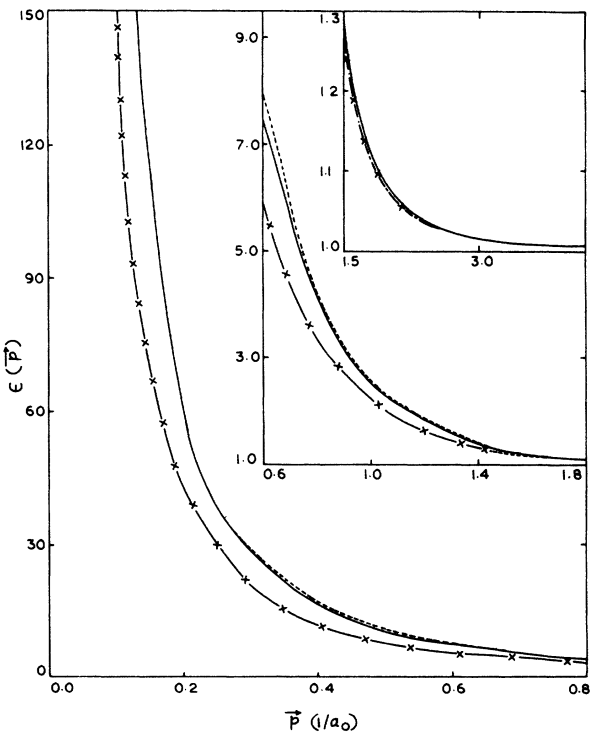


FIG. 6. $\epsilon(\vec{p})$ vs $\vec{p}$ for copper. The solid lines represents $\epsilon(\vec{p})$ in the [100] direction, and the dashed lines represents $\epsilon(\vec{p})$ along the [110] direction. $\epsilon(\vec{p})$ along the [111] direction almost coincides with the dashed line. For $p > 1.5$, the dashed line and the solid line also coincide. The cross-dashed line represents the unscreened $\epsilon(\vec{p})$ [Eq. (1)] along the [100] direction. In the upper-right-hand corner, $\epsilon(\vec{p})$ is shown on the magnified scale.

$$\det \left| D_{\alpha\beta}(\vec{q}) - M\omega_{q\rho}^2 \delta_{\alpha\beta} \right| = 0 \ . \qquad (17)$$

Here the subscript $p$ denotes the polarization branch, $M$ is the mass of the ion, $D_{\alpha\beta}(\vec{q})$ are the elements of the dynamical matrix, and $\alpha, \beta$ are the Cartesian components $(x, y, z)$. $D_{\alpha\beta}(\vec{q})$ is written as the sum of the three terms[32]:

$$D_{\alpha\beta}(\vec{q}) = D_{\alpha\beta}^{(C)}(\vec{q}) + D_{\alpha\beta}^{(R)}(\vec{q}) + D_{\alpha\beta}^{(E)}(\vec{q}) \ . \qquad (18)$$

$D_{\alpha\beta}^{(C)}(\vec{q})$ arises from the electrostatic interaction between the ions, $D_{\alpha\beta}^{(R)}(\vec{q})$ originates from the overlap interaction between the ion cores, and $D_{\alpha\beta}^{(E)}(\vec{q})$ stems from the ion-electron-ion interaction which also includes electron-electron interactions. $D_{\alpha\beta}^{(C)}(\vec{q})$ is evaluated by Ewald's $\Theta$-function transformation for unit ionicity and fcc crystal structure. The ion cores of noble metals are sufficiently large as compared to sodium, therefore the contribution of $D_{\alpha\beta}^{(R)}(\vec{q})$ to the phonon frequencies may not be negligible. Toya[1] had used Born-Mayer exchange-overlap potential which is suitable only for the ionic crystals where the core wave functions of the negative ion are sufficiently spread out.[33] In a recent paper Moriarty[11] calculated explicitly the exchange-overlap potential between ion cores for all the noble metals and represented it by a simple analytical expression

$$v_{01}(R) = s[1 + l(R/R_{nn} - 1) + t\,l^2(R/R_{nn} - 1)^2] \times e^{-u(R/R_{nn}-1)} \ , \qquad (19)$$

where $R_{nn}$ is the first-nearest-neighbor distance, and the four parameters $s, l, t$, and $u$ are determined by calculating explicitly $v_{01}(R)$ and its first and second derivatives at $R_{nn}$, and $v_{01}(R)$ at the second-nearest-neighbor distance. These parameters are tabulated by Moriarty.[11] Using (19), $D_{\alpha\beta}^{(R)}(\vec{q})$ can easily be evaluated and the final expression for the contribution to the phonon frequencies due to $D_{\alpha\beta}^{(R)}(\vec{q})$ can be written:

$$\omega_{q\rho}^2(R) = \omega_{p1}^2 \frac{\Omega_0}{4\pi z e^2} \sum_{\alpha\beta} \sum_{L}{}' \left[ \frac{s}{R_{nn}^2} (uT + 2t\,l^2) \frac{L_\alpha L_\beta}{L^2} + \frac{sS}{LR_{nn}} \left( \delta_{\alpha\beta} - \frac{L_\alpha L_\beta}{L^2} \right) \right] e^{-u(L/R_{nn}-1)} \times [1 - \cos(\vec{q}\cdot\vec{L})] e_{q\rho\alpha} e_{q\rho\beta} \ , \qquad (20)$$

where

$$T = u - 2l - (4sl^2 - ul)(L/R_{nn} - 1) + utl^2(L/R_{nn} - 1)^2 \qquad (21)$$

and

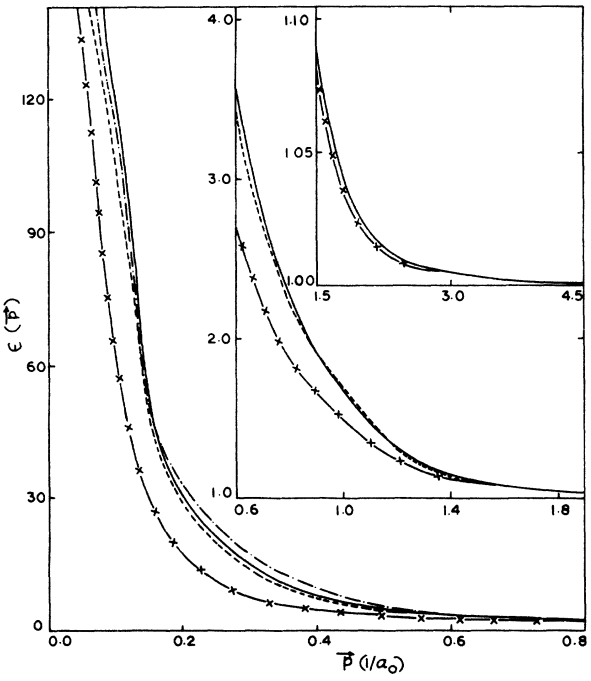


FIG. 7. $\epsilon(\vec{p})$ vs $\vec{p}$ for silver. The solid, dashed, and dash-dot lines represent $\epsilon(\vec{p})$ along [100], [110], and, [111] directions, respectively. For $1.5 > p > 0.6$, the solid and the dash-dot lines coincide, while for $p > 1.5$, all the three lines coincide. The cross-dash line represents unscreened $\epsilon(\vec{p})$ [Eq. (1)] along the [100] direction. In the upper-right-hand corner, $\epsilon(\vec{p})$ is shown on the magnified scale.

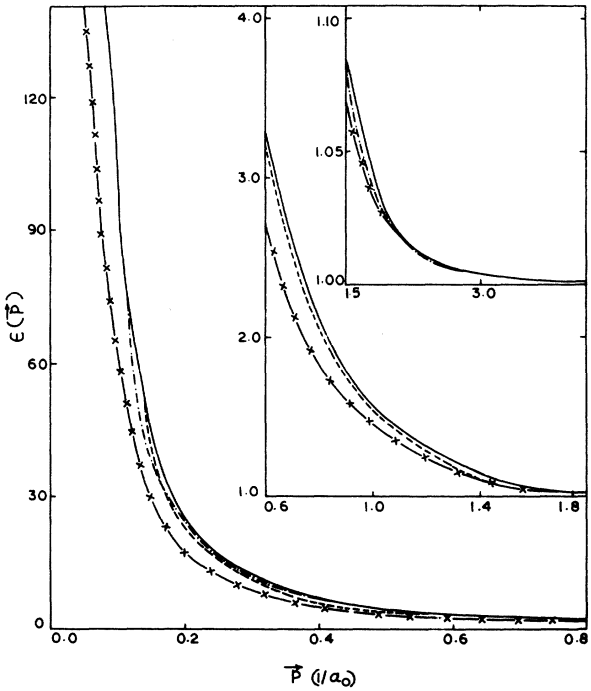


FIG. 8. $\epsilon(\vec{p})$ vs $\vec{p}$ for gold. The description is the same as that of Fig. 7. For $1.8 > p > 0.6$, $\epsilon(\vec{p})$ along the [111] direction coincides with the solid line.

$$S = -u + l + (2tl^2 - ul)(L/R_{nn} - 1) - utl^2(L/R_{nn} - 1)^2 . \quad (22)$$

The lattice vector $\vec{L} = \frac{1}{2}a_l(L_x, L_y, L_z)$, where $a_l$ is lattice parameter, and the plasma frequency $\omega_{pl} = (4\pi z^2 e^2/M\Omega_0)^{1/2}$. The prime over $\sum$ denotes that the term $\vec{L}=0$ is excluded. $e_{q\rho\alpha}$ and $e_{q\rho\beta}$ are the $\alpha$ and $\beta$ components of the polarization vector $\vec{e}_{q\rho}$. The sum over $\vec{L}$ is done only for the first and second nearest neighbors.

The contribution, due to $D^{(g)}_{\alpha\beta}(\vec{q})$, to the phonon frequencies is evaluated in paper II. The final expression is written

$$\omega^2_{q\rho}(E) = \frac{N}{M}\Bigg[\sum_G [\vec{e}_{q\rho}\cdot(\vec{q}+\vec{G})]^2 \frac{1}{v(\vec{q}+\vec{G})} \times\left(\frac{1}{\epsilon(\vec{q}+\vec{G})}-1\right)|U_b(\vec{q}+\vec{G})|^2 - \sum_{G\neq 0}[\vec{e}_{q\rho}\cdot\vec{G}]^2 \times\frac{1}{v(\vec{G})}\left(\frac{1}{\epsilon(\vec{G})}-1\right)|U_b(\vec{G})|^2\Bigg] . \quad (23)$$

$N$ is the number of ions in the crystal, $v(\vec{p})$ and $U_b(\vec{p})$ are the Fourier transforms of Coulomb interaction between the electrons and the bare-electron–ion potential, respectively. As pointed out in paper II, the phonon frequencies become imaginary if the bare-electron–ion potential calculated by the Hartree-Fock-Slater self-consistent scheme is used. This is because of the fact that the $s$ and $d$ wave functions, which have been used to calculate the dielectric function, are neither mutually orthogonal nor orthogonal to the core wave functions. An explicit inclusion of the orthogonality of these wave functions leads to involved calculations. Therefore, the simple Harrison-model[34] potential is used for the bare-ion potential. This simplifies Eq. (23) as

$$\omega^2_{q\rho}(E) = -\omega^2_{pl}\Bigg(\sum_G \frac{[\vec{e}_{q\rho}\cdot(\vec{q}+\vec{G})]^2}{|\vec{q}+\vec{G}|^2}F(\vec{q}+\vec{G}) - \sum_{G\neq 0}\frac{[\vec{e}_{q\rho}\cdot\vec{G}]^2}{|\vec{G}|^2}F(\vec{G})\Bigg) , \quad (24)$$

where

$$F(\vec{p}) = \left(\frac{\epsilon(\vec{p})-1}{\epsilon(\vec{p})}\right)\left[-1+\frac{p^2}{4\pi z e^2}\frac{\beta_c}{[1+(pr_c)^2]^2}\right] . \quad (25)$$

The first term in the large square bracket in Eq. (25) arises from the Coulomb potential due to net ionic charge, and the second term represents the repulsive interaction between the core and the conduction electrons. The parameters $\beta_c$ and $r_c$ represent the strength of this repulsive interaction.

It is a prohibitively difficult task to include explicitly $\epsilon_{ds}(\vec{p})$ to calculate the phonon frequencies for a set of phonon wave vectors. Therefore, we average the $\epsilon_{ds}(\vec{p})$ by Houston's method and represent averaged $\epsilon_{ds}(\vec{p})$ by an analytic function

$$\epsilon^{av}_{ds}(p) = -\frac{2m_s k_d e^2 f_c}{\pi\hbar^2 p^2}\left[1+\frac{4k_d^2-p^2}{4k_d p}\ln\left|\frac{2k_d+p}{2k_d-p}\right|\right] . \quad (26)$$

The parameters $f_c$ and $k_d$ are chosen in such a way that $\epsilon^{av}_{ds}(p)$ is in closest agreement with its detailed calculations. The values of $(k_d, f_c)$ are (0.638, 1.00), (0.53, 0.0187), and (0.54, 0.273) for copper, silver, and gold, respectively. Therefore, the dielectric function which is finally used in the calculation of phonon frequencies is

$$\epsilon(p) = 1 - \epsilon'_{ss}(p) - \epsilon^{av}_{ds}(p) . \quad (27)$$

The phonon frequencies of noble metals are calculated using Eqs. (29), (24), and (27). The sum over $\vec{G}$ in Eq. (24) is taken for 259 nearest-reciprocal-lattice vectors. The parameters $\beta_c$ and $r_c$ for copper and silver are obtained in such a manner that the normalized energy wave-number characteristic function $F(p)$ converges within the range of summation over $\vec{G}$ and agreement between the calculated and experimental phonon frequencies is achieved in the longitudinal branch in the [100] direction at the zone boundary. The values of these parameters $(\beta_c, r_c)$ are (11.10, 0.257) and (10.50, 0.17) for copper and silver, respectively. Using these values of $\beta_c$ and $r_c$, the phonon frequencies of copper and silver are calculated along the three principal symmetry directions [100], [110], and [111]. The results for copper are compared with the experimental values of Nicklow *et al.*[35] in Fig. 9, while the results for silver are compared with the experimental values of Kamitakahara and Brockhouse[36] in Fig. 10. The phonon frequencies for copper are in fairly good agreement with the experimental values except for the transverse branches in the [100] and [110] directions. The maximum deviation is 18%. Comparing the results for copper with those obtained in paper III, we find that the phonon frequencies of the transverse branches are enhanced by 30% at the maximum. This emphasizes that the overlap potential between the ion cores for noble metals should not be completely neglected. The Kohn anomalies as pointed out by Moriarty in the $T$ and $T_1$ branches in [100] and [110] directions, respectively, are not found in our calculations. The results for silver are in fairly good agreement with the experimental values. The maximum deviation is less than 10% in the longitudinal and transverse branches in [100] direction for intermediate values of $\vec{q}$. A similar analysis of the phonon frequencies of silver is also done by Drexel,[37] but he uses Born-Mayer exchange-overlap potential and the Hartree dielectric function, which are hardly justified for noble metals.

The experimental phonon frequencies for gold are not available. Therefore, the parameters $\beta_c$

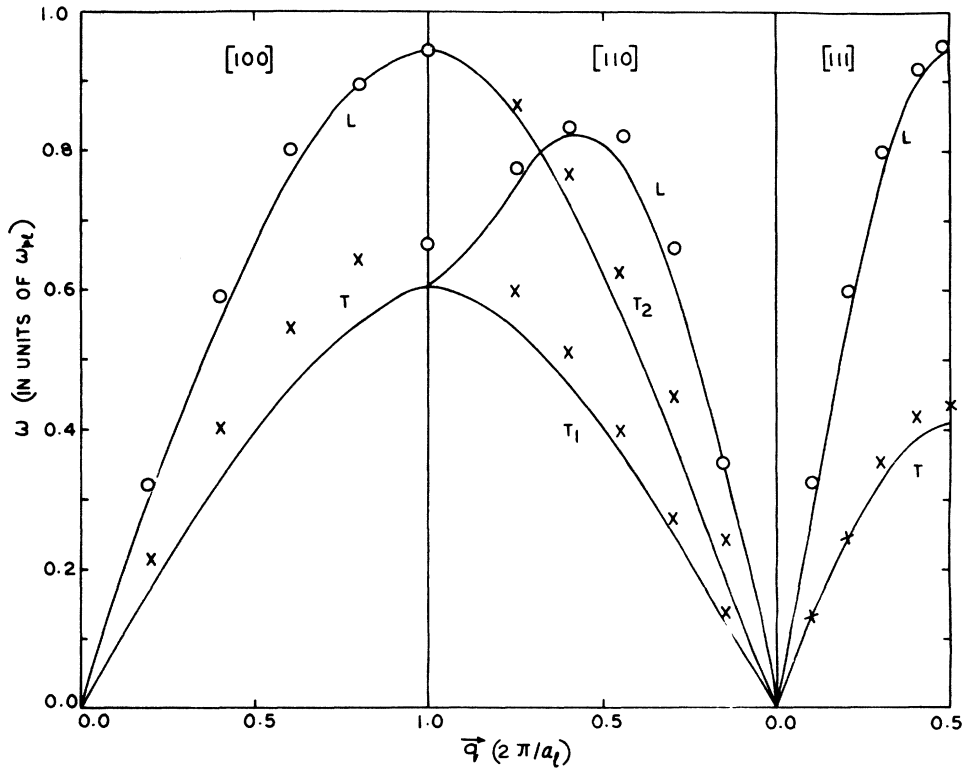


FIG. 9. $\omega(\vec{q})$ vs $\vec{q}$ for copper. The solid lines represent the present calculations. Open circles and the crosses represent the experimental values for longitudinal and the transverse branches, respectively.

and $r_c$ for gold are obtained by matching the calculated phonon frequencies with the calculations of Moriarty at $\vec{q} = (2\pi/a_l)$ (0.1, 0.1, 0.1) because the phonon frequencies of silver due to Moriarty are in fairly good agreement with the experimental values for this particular wave vector. The parameters $\beta_c$ and $r_c$ are 3.00 and 0.15, respectively, for gold. The calculated phonon frequencies along

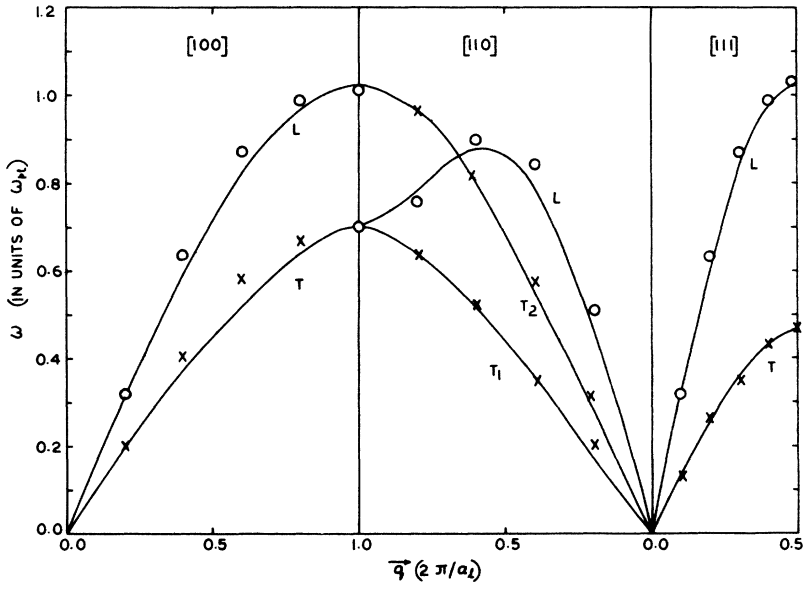


FIG. 10. $\omega(\vec{q})$ vs $\vec{q}$ for silver. The description is the same as that of Fig. 9.

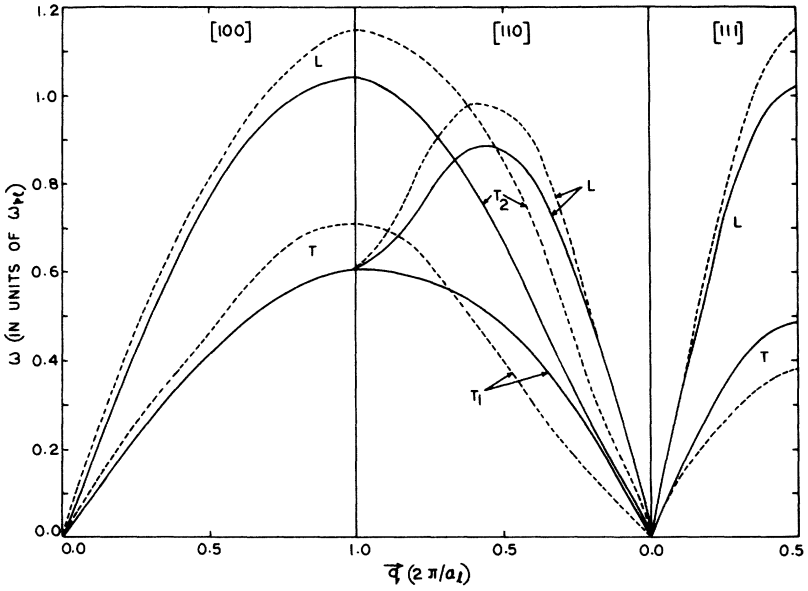


FIG. 11. $\omega(\vec{q})$ vs $\vec{q}$ for gold. The solid lines represent the present calculations, while the dashed lines represent the calculations of Moriarty (Ref. 11).

all the symmetry directions are compared with the calculations of Moriarty in Fig. 11. The phonon frequencies due to Moriarty are higher than the present calculations for large values of $\vec{q}$.

The normalized energy wave-number characteristic functions $F(p)$ are shown in the Fig. 12. For the sake of comparison, the function $F(p)$ for copper due to Moriarty is also presented there. We find that the qualitative behavior of the present calculations is the same as that of Moriarty except for a sharp hump near $2k_{Fs}$. The qualitative behavior of the function $F(p)$ is the same for all the noble metals. The function $F(p)$ decreases more rapidly for gold as compared to that of copper and silver for large values of $p$. The function $F(p)$ for silver is less than that of copper in the low-$p$ region.

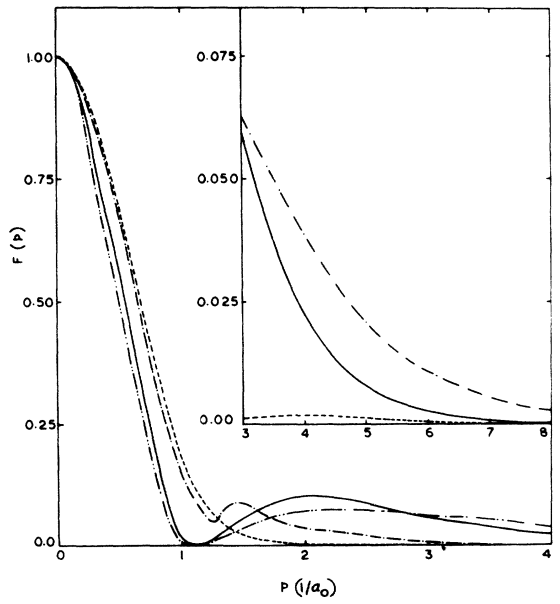


FIG. 12. The function $F(p)$ vs $p$. The solid, dash-double-dot, and dashed lines represent the results for copper, silver, and gold, respectively. The dash-dot line represent the calculations of Moriarty (Ref. 11) for copper. In the upper-right-hand corner the results are shown on the magnified scale.

## V. EFFECTIVE INTERACTION BETWEEN IONS

The effective interaction between ions is taken as the sum of the three contributions in the present

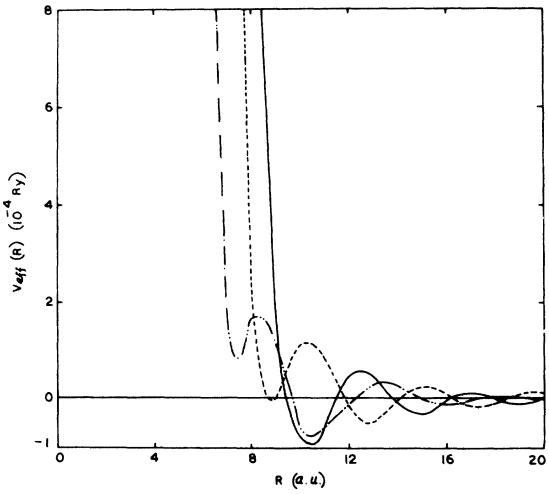


FIG. 13. $V_{eff}$ $(R)$ vs $R$ for noble metals. The description is the same as that of Fig. 12.

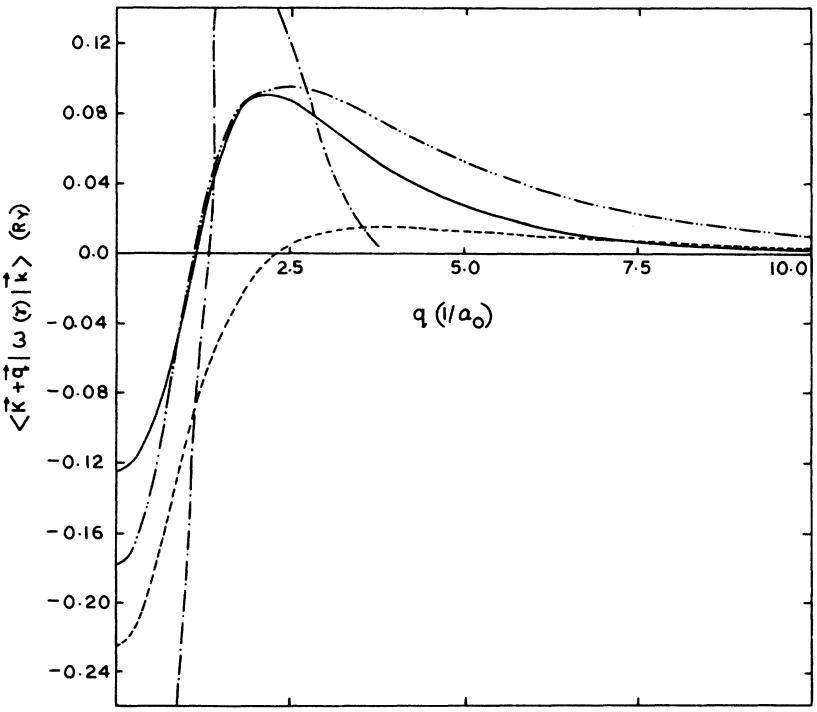


FIG. 14. Form factors for noble metals. The description is the same as that of Fig. 12.

scheme as discussed in an earlier section. We, therefore, write

$$v_{\rm eff}(R)=\frac{z^2e^2}{R}+v_{\rm ol}(R) -\frac{4z^2e^2}{\pi}\int F(p)\frac{\sin pr}{pr}\,dp\ . \qquad (28)$$

The first and second terms represent the Coulomb and overlap potentials between ions and the third term represents the effective electron-ion interaction. The calculated values of $v_{\rm eff}(R)$ are shown in the Fig. 13. The first minimum of $v_{\rm eff}(R)$ lies in the vicinity of fifth, fourth, and third nearest neighbors for copper, silver, and gold, respectively. This could be expected as $v_{\rm eff}(R)$ is not the actual effective interaction between the ions. The volume-dependent terms should also be included in (28). The mutual cancellation of the attractive and the repulsive parts of (28) starts beyond fourth-neighbor distance for copper, while it starts beyond third-neighbor distance for silver and gold. These oscillations of $v_{\rm eff}(R)$ are the familiar Friedel oscillations which arise from the sharp cutoff of the electron distribution function at the Fermi momentum. Because of very rapid decrease of $v_{\rm ol}(R)$, $v_{\rm eff}(R)$ for silver shows a small dip at $r=7.5$ bohr.

## VI. FORM FACTORS

The screened form factor

$$\langle\vec{k}+\vec{p}\,|w(r)|\,\vec{k}\rangle=\left(-\frac{4\pi ze^2}{p^2}+\frac{\beta_c}{[1+(pr_c)^2]^2}\right) \times\frac{1}{\Omega_0\epsilon(p)}\ , \qquad (29)$$

where $\epsilon(p)$ is given by Eq. (27) and $w(r)$ is the Harrison's screened-model potential. In the limit $p\to 0$, the right-hand side of Eq. (29) simplifies to

$$-\frac{1}{\Omega_0}\left(\frac{\pi^2z\hbar^2}{m_s(k_{Fs}C_s+f_ck_d)}\right)\ ,$$

where

$$C_s=\left(1-\frac{4ABM_se^2}{\pi\hbar^2k_{Fs}}\right)^{-1}\ .$$

The form factors for all the noble metals are calculated with the help of Eq. (29). These form fac-

TABLE V. Binding energy of noble metals in rydbergs.

| | Copper | Silver | Gold |
|---|---|---|---|
| $E_{\rm es}$ | −0.672 | −0.595 | −0.597 |
| $E_{\rm ol}$ | 0.049 | 0.032 | 0.070 |
| $E_0$ | 0.309 | 0.243 | 0.245 |
| $E_x$ | −0.342 | −0.304 | −0.305 |
| $E_c$ | −0.086 | −0.082 | −0.082 |
| $E_1$ | 0.278 | 0.183 | 0.052 |
| $E_{\rm bs}$ | −0.135 | −0.130 | −0.019 |
| $E_{\rm BI}$(theor.) | −0.599 | −0.653 | −0.636 |
| $E_{\rm BI}$(Ref. 11) | −0.800 | −0.649 | −0.652 |
| $E_{\rm BI}$(expt.)[a] | −0.826 | −0.775 | −0.957 |

[a]Experimental binding energy is equal in magnitude to the cohesive energy plus the first ionization energy of the free atom.

tors are shown in the Fig. 14. In the low-$p$ region, our calculated values for copper are higher than those of Moriarty because we use a different dielectric function. Our form factors fall off more slowly than the Moriarty form factor. The estimated band gaps are 0.14 and 0.16 Ry at the $L$ symmetry point for copper and silver, while the experimental values[38] are 0.35 and 0.28 Ry, respectively. The band gap for gold at the $L$ symmetry point becomes rather unphysical. The general behavior of the form factors for copper and silver is the same while it is more negative for gold. The two contributions of the form factor become equal at $p = 1.2$ for copper and silver and at $p = 2.3$ for gold.

## VII. COHESIVE ENERGY

The cohesive energy per particle for a neutral atom is given as

$$E_{\mathrm{coh}} = E_I + E_{\mathrm{BI}} , \tag{30}$$

where $E_I$ is the first ionization energy and the binding energy[39]

$$E_{\mathrm{BI}} = E_{es} + E_{ol} + E_0 + E_x + E_c + E_1 + E_{bs}$$

$$= -\frac{z^2 e^2 \bar{\alpha}}{(3\Omega_0/4\pi)^{1/3}} + \frac{1}{2}\sum_i{}' v_{ol}(R_i) + \tfrac{3}{5} z E_F - \frac{3}{4\pi} z e^2 k_{Fs}$$

$$+ z\left(-0.112 + 0.0335 \ln \bar{r}_s - \frac{0.02}{0.1 + \bar{r}_s}\right) + \sum_{k \le k_{Fs}} \langle \vec{k} \left| w_0(r) + \frac{z e^2}{r} \right| \vec{k} \rangle + \sum_G F(\vec{G})(4\pi z^2 e^2/\Omega_0 G^2) .$$

The first term is the electrostatic energy of the ions. $\bar{\alpha}$ is the Madelung constant which is 1.7917 for fcc lattice. The second term is the same as calculated by Moriarty. The third and the fourth terms represent the average kinetic energy and the exchange energy. Fifth term is the correlation energy which has been taken from a recent calculation of Vashishta and Singwi.[28] The sixth term represents the core-conduction repulsive energy and the last term represents the so-called band-structure energy. The sum in the last term is taken over 500 reciprocal-lattice vectors where $F(\vec{G})$ becomes practically zero. The calculated values of binding energy are tabulated in Table V. The agreement between the calculated values and the experimental values is rather poor. But our calculated values agree with the calculations of Moriarty for silver and gold, while for copper our results are lower than Moriarty. This is because of the fact that in the present scheme the contribution of free-electron energy to the total energy is large for copper as compared to that of silver and gold and the cohesive energy is quite sensitive to free-electron energy.

## VIII. CONCLUSIONS

In these calculations a rather simplified picture of noble metals is used. The detailed band-structure calculations are incorporated in the noninteracting band scheme to calculate the dielectric function. The hybridization of the $s$ and $d$ bands is not rigorously taken into account, because that leads to an involved calculation. The exchange-correlation corrections to the $s$-$s$ part of the dielectric function are included in a rather phenomenological way from the prescriptions of Singwi *et al.* The calculated phonon frequencies for copper and silver are in reasonably good agreement with the experimental values. The overlap potential which we incorporated from the detailed calculations of Moriarty, enhances the phonon frequencies in the transverse branches. The form factors and the energy wave-number characteristic functions, which may be useful to calculate many additional physical properties of these metals, can easily be reproduced. The effective ion-ion potentials for these metals show the correct oscillatory behavior for large distance. The calculated binding energy is in rather poor agreement with the experimental values but it shows a reasonable agreement with the results of Moriarty which involve heavy computations. The relativistic effects for gold may be quite important. Anharmonic effects have also been neglected. A rigorous inclusion of $s$-$d$ hybridization and a more accurate calculation of overlap potential may further improve the results.

## ACKNOWLEDGMENTS

We thankfully acknowledge very helpful discussions with Professor S. K. Joshi and Dr. K. N. Pathak. We wish to thank Dr. E. C. Snow for supplying his data for the energy-band calculations of silver. The financial assistance from the Council of Scientific and Industrial Research and from the University Grants Commission is also acknowledged.

[1]T. Toya, J. Res. Inst. Catal. Hokkaido Univ. **9,** 178 (1961); Prog. Theor. Phys. **20,** 974 (1958).
[2]T. Toya, in *Lattice Dynamics*, edited by R. F. Wallis (Pergamon, New York, 1965), p. 91.
[3]S. K. Sinha, Phys. Rev. **169,** 477 (1968).
[4]D. C. Golibersuch, Phys. Rev. **157,** 532 (1967).
[5]S. Das, Phys. Rev. B 7, 2238 (1973).
[6]D. Nowak, Phys. Rev. B **6,** 369 (1972).
[7]F. M. Mueller, Phys. Rev. **153,** 659 (1967).
[8]J. M. Ziman, Proc. Phys. Soc. Lond. **86,** 337 (1965).
[9]W. A. Harrison, Phys. Rev. **181,** 1036 (1969).
[10]J. A. Moriarty, Phys. Rev. B **1,** 1363 (1970).
[11]J. A. Moriarty, Phys. Rev. B **6,** 1239 (1972).
[12]V. K. Nikulin and M. B. Trihaskovskaya, Phys. Status Solidi **28,** 801 (1968); A. I. Gubanov and V. K. Nikulin, Phys. Status Solidi **17,** 815 (1966); V. K. Nikulin, Fiz. Tverd. Tela **7,** 2708 (1965) [Sov. Phys.-Solid State **7,** 2189 (1966)]; Phys. Lett. A **36,** 337 (1971).
[13]P. Gombas, Acta Phys. **1,** 301 (1952).
[14]V. Heine and I. V. Avarenkov, Philos. Mag. **9,** 451 (1964).
[15]J. Hubbard, Proc. R. Soc. A **243,** 336 (1958).
[16]L. Kleinman, Phys. Rev. **160,** 585 (1967).
[17]S. Prakash and S. K. Joshi, Phys. Rev. B **2,** 915 (1970).
[18]S. Prakash and S. K. Joshi, Phys. Rev. B **4,** 1770 (1971).
[19]S. Prakash and S. K. Joshi, Phys. Rev. B **5,** 2880 (1972).
[20]K. S. Singwi, M. P. Tosi, R. H. Land, and A. Sjölander, Phys. Rev. **176,** 589 (1968); Phys. Rev. B **1,** 1044 (1970).
[21]E. C. Snow and J. T. Waber, Phys. Rev. **157,** 570 (1967).
[22]E. C. Snow, Phys. Rev. **172,** 708 (1968).
[23]N. E. Christensen and B. O. Seraphin, Phys. Rev. B **4,** 3321 (1971).
[24]R. E. Watson, MIT Report, 1958 (unpublished).
[25]F. Herman and S. Skillman, *Atomic Structure Calculations* (Prentice-Hall, Englewood Cliffs, N.J., 1963).
[26]J. B. Scarborough, *Numerical Mathematical Analysis*, 6th ed. (IBH, Bombay, 1966).
[27]S. Prakash and S. K. Joshi, Phys. Rev. **185,** 915 (1969).
[28]P. Vashishta and K. S. Singwi, Phys. Rev. B **6,** 875 (1972); Phys. Rev. B **6,** 4883 (1972).
[29]W. Kohn and L. J. Sham, Phys. Rev. **140,** A1133 (1965).
[30]I. Lindgren, Int. J. Quantum Chem. **5,** 411 (1971).
[31]L. Hedin, Ark. Fys. **30,** 231 (1965).
[32]S. K. Joshi and A. K. Rajagopal, Solid State Phys. **22,** 159 (1968).
[33]S. H. Vosko, Phys. Lett. **13,** 97 (1964).
[34]W. A. Harrison, *Pseudopotentials in the Theory of Metals* (Benjamin, New York, 1966).
[35]R. M. Nicklow, G. Gilat, H. G. Smith, L. J. Raubenheimer, and M. K. Wilkinson, Phys. Rev. **164,** 922 (1967).
[36]W. A. Kamitakahara and B. N. Brockhouse, Phys. Lett. A **29,** 639 (1969).
[37]W. Drexel, Z. Phys. **255,** 281 (1972).
[38]G. P. Pells and M. Shiga, J. Phys. C **2,** 1835 (1969), for copper; J. F. Cornwall, Philos. Mag. **6,** 727 (1961).
[39]T. Schneider and E. Stoll, in *Neutron Inelastic Scattering* (International Atomic Energy Agency, Vienna, 1968), Vol. 1, p. 101.